THE JOURNAL OF BIOLOGICAL CHEMISTRY
Vol. 280, No. 16, Issue of April 22, pp. 15690–15699, 2005
Printed in U.S.A.

Association States of Nucleosome Assembly Protein 1 and Its Complexes with Histones*

Received for publication, November 26, 2004, and in revised form, January 10, 2005
Published, JBC Papers in Press, January 31, 2005, DOI 10.1074/jbc.M413329200

Katalin Fejes Tóth‡§, Jacek Mazurkiewicz‡, and Karsten Rippe‡¶

From the ‡Kirchhoff-Institut für Physik, AG Molekulare Biophysik, Ruprecht-Karls-Universität Heidelberg, Im Neuenheimer Feld 227 and the §Deutsches Krebsforschungszentrum, Abt. Molekulare Genetik (B060), Im Neuenheimer Feld 280, D-69120 Heidelberg, Germany

The histone chaperone NAP1 is a carrier of histones during nuclear import, nucleosome assembly, and chromatin remodeling. Analytical ultracentrifugation was used to determine the association states of NAP1 alone and in complexes with core histones. In addition, the concentration dependence of the association was quantified by determining the equilibrium dissociation constant between different NAP1 species. At physiological protein and salt concentrations the prevalent species were the NAP1 dimer and octamer. These were also the association states found to interact with histones in a stoichiometry of one NAP1 monomer per histone. Based on these results a model for a cell cycle-dependent shift of the NAP1 dimer-octamer equilibrium is proposed that reflects different biological functions of NAP1.

In eukaryotes the DNA is packed into nucleosomes consisting of 147 bp of DNA wrapped around an octamer of small basic histone proteins (1–4). This octamer consists of two copies of histones H2A, H2B, H3, and H4, respectively. The nucleosome constitutes the basic repeating unit of chromatin, and formation of a regularly spaced nucleosome chain during chromatin assembly is a prerequisite to maintain the biological activity of chromatin. This requires ATP-dependent chromatin assembly factors as well as so-called histone chaperones (5–10). Histone chaperones bind histone proteins and prevent nonspecific, charge-based interaction with nucleic acids. This activity appears essential to cell viability, because simple mixing of histones and DNA *in vitro* at physiological salt concentrations leads to the rapid formation of poorly defined insoluble aggregates (11, 12). One of these chaperones, the nucleosome assembly protein 1 (NAP1)[1] (13, 14), is involved in the transport of the histone H2A·H2B dimer from the cytoplasm to the nucleus and the deposition of histones onto the DNA as described in several reviews (5–7, 10). NAP1 is highly acidic, which is likely to mediate its interaction with the positively charged histone proteins. It is thought to function in large chromosomal domains rather than at local restricted sites (5), and in yeast loss of NAP1 leads to an altered gene expression of about 10% of the genome (15). NAP1 is present at micromolar concentrations throughout the cell cycle, and an increase of the NAP1 concentration during S-phase has been reported for some NAP1 homologues in higher eukaryotes (16–19). Various lines of evidence indicate that NAP1 and the related NAP2 protein are mainly cytoplasmic during G_1 and G_2 phase with only a small fraction in the nucleus and translocate into the nucleus during S phase (14, 19–21).

In vivo experiments show coimmunoprecipitation of NAP1 with the histones H2A and H2B but not with H3 and H4 (11, 22). In contrast, NAP1 is capable of binding all four core histones *in vitro* (13, 14, 23–25). Several studies focused on the determination of the association state of NAP1, which in yeast has a monomer molecular mass of 47.9 kDa. By gel filtration or gradient centrifugation very different molecular masses ranging from 120 to 600 kDa and sedimentation coefficients from 1.5 S up to 7 S were reported. In a recent study it was concluded based on analytical ultracentrifugation experiments that yNAP1 exists as complex mixture of species with *s* values between 4.5 and 12 S at physiological salt concentrations (75 and 150 mM NaCl). In the presence of 500 mM NaCl concentration a 4.5 S NAP1 dimer was identified (26). It appears that upon mixing NAP1 with histones distinct complexes are formed, which sediment around 5–6 S, 8 S, and 10–12 S, respectively (13, 23, 24). Within the 12 S complex all four histones cosedimented in nearly equal amounts, and upon addition of DNA nucleosomes were formed. The 5–6 S complex was assigned to a NAP1 complex with the H2A·H2B dimer and the 8 S complex to a complex that contains NAP1 and the $(H3{\cdot}H4)_2$ tetramer (13, 23, 24). Hence, the biologically highly relevant interaction of NAP1 with histones appears to be tightly connected to the NAP1 association state. In particular, the nature of the different NAP1 complexes observed previously at physiological ionic strength and their relation to specific NAP1 activities remain to be elucidated.

Here, we have used analytical ultracentrifugation (AUC) to determine the different association states of NAP1 on its own and in complexes with histones. AUC is very useful for the identification of the oligomeric state and the stoichiometry of proteins, and to characterize their thermodynamic and hydrodynamic properties in solution (27, 28). The concentration dependence of the equilibrium between different NAP1 species was quantified in terms of the corresponding dissociation constants. At physiological protein and salt concentrations the dominating species were the NAP1 dimer and octamer, which were also the association states found to interact with histones. Based on these results and estimates of the intracellular concentration of NAP1 we propose a model, in which the transport/exchange of H2A·H2B dimers in G_1 and G_2 phase is mediated by NAP1 dimers. The accumulation of NAP1 in the nucleus during S phase induces the association of NAP1 into an octamer complex. This species has eight histone binding sites so that it could act as a carrier for multiple histone dimers as required for the *de novo* assembly of nucleosomes.

* The costs of publication of this article were defrayed in part by the payment of page charges. This article must therefore be hereby marked "*advertisement*" in accordance with 18 U.S.C. Section 1734 solely to indicate this fact.

¶ To whom correspondence should be addressed. Tel.: 49-6221-54-9270; Fax: 49-6221-54-9112; E-mail: Karsten.Rippe@kip.uni-heidelberg.de.

[1] The abbreviations used are: NAP1, nucleosome assembly protein 1; AUC, analytical ultracentrifugation; *s*, sedimentation coefficient; *D*, diffusion coefficient.

EXPERIMENTAL PROCEDURES

Expression and Purification of NAP1—Yeast NAP1 was expressed from plasmid pET28-yNAP1 from Toshio Tsukiyama with a N-terminal His tag. The plasmid corresponds to *Saccharomyces cerevisiae* NAP1 with a T7 tag cloned into the NdeI site of pET28a. The His tag is followed by a thrombin cleavage site. The expressed NAP1 protein has a calculated molecular mass of 52.4 kDa with the His tag and 49.5 kDa after thrombin cleavage. Protein overexpression from pET28-yNAP1 was in *Escherichia coli* BL21(DE3) carrying the pLysS plasmid. For purification, cells were suspended in lysis buffer (20 mM Tris-HCl, pH 7.5, 500 mM KCl, 20 mM imidazole, 5 mM mercaptoethanol, 15% glycerol, 1 mM EDTA, 0. 1% Nonidet P-40, 1 mM Pefabloc), sonicated, and centrifuged. Nickel-agarose beads were equilibrated with lysis buffer and added to the supernatant after supplementing $MgCl_2$ to a final concentration of 2 mM. Binding was allowed for 3–4 h at 4 °C, and beads were washed twice with lysis buffer and twice with washing buffer (20 mM Tris-HCl, pH 7.5, 100 mM KCl, 20 mM imidazole, 5 mM mercaptoethanol, 15% glycerol, 0.01% Nonidet P-40, 1 mM Pefabloc). Elution was conducted with washing buffer supplemented with 0.5 M imidazole. The eluate was dialyzed against buffer A (20 mM Tris-HCl, pH 7.5, 100 mM M KCl, 1 mM dithiothreitol, 10% glycerol, 0.1 mM EDTA). The protein was further purified on a Mono-Q column and eluted with a KCl gradient from 0.1 to 1 M in buffer A. Fractions were checked on SDS-PAGE, and NAP1-containing fractions were pooled and dialyzed against buffer A. DNase activity was tested by incubating NAP1 with supercoiled plasmid DNA over 2 days. For some experiments the His tag was removed by binding purified NAP1 to nickel-agarose and incubating with biotin-tagged thrombin for 2 h at 20 °C using the thrombin cleavage kit according to the specifications given by the manufacturer (Novagen, Madison, WI). Thrombin was subsequently removed with streptavidin beads. Using the program SEDNTERP[2] (29) the monomer extinction coefficient of NAP1 was calculated from the amino acid sequence to be ϵ_{280} = 37,000 $M^{-1}\cdot cm^{-1}$. From the absorbance spectrum of the protein we derived the corresponding value of ϵ_{230} = 293,000 $M^{-1}\cdot cm^{-1}$.

Preparation and Gel Electrophoresis Analysis of Fluorescent Histone Complexes—Recombinant *Xenopus laevis* histones H2A12C, H2B, H3C110A, and H4K5C were overexpressed from pET plasmids in *E. coli* as described previously (30, 31). The H2A12C and H4K5C proteins contain a cysteine substitution, allowing specific labeling with thiol-reactive probes (32, 33). In Histone H3C110A the cysteine is substituted against alanine to hinder modification of this residue, which could lead to functional impairment. Histones H2A12C and H2B or H3C110A and H4K5C were dissolved in unfolding buffer containing 7 M guanidinium chloride, 20 mM Tris-HCl, pH 7.5, 1 mM EDTA, and 5 mM mercaptoethanol at equimolar ratios and a total protein concentration of 1 mg/ml. Refolding was by dialysis into the same buffer but without guanidinium chloride. A reducing agent was removed by repeated concentration and dilution of histone proteins in freshly degassed labeling buffer (20 mM Tris-HCl, pH 7.2, 0.1 mM EDTA) using Vivaspin 20 concentrators (Vivascience, Hannover, Germany). Labeling was carried out at a histone monomer concentration of ~60 μM with a 1.5 times molar excess of Alexa Fluor 488 C5 maleimide (Molecular Probes Europe BV, Leiden, Netherlands) for 1 h. The reaction was stopped by adding 10 mM dithiothreitol and incubating for 30 min on ice. Labeled histone complexes were then purified from misfolded histone and free dye using BioRex 70 resin (Bio-Rad Laboratories GmbH) as described before (32). Concentration of labeled histones and labeling efficiency were assessed by absorbance spectroscopy using an excitation coefficient of ϵ_{496} = 72,000 $M^{-1}\cdot cm^{-1}$ for the Alexa 488 label (34) and the published values for the histones at a wavelength of 276 nm (30) after subtracting the contribution of Alexa 488 at this wavelength. A labeling efficiency of 70% was routinely reached for H2A12C and 50% for H4K5C, and the labeled histones behaved identically to the wild type in terms of association state. Agarose gel electrophoresis of NAP1 complexes with labeled histones was conducted on 1% agarose gels in 0.11× TBE (10 mM Tris, 10 mM boric acid, 0.22 mM EDTA) supplemented with 10 mM KCl. NAP1 and histones were mixed prior to loading in 10 mM Tris-HCl, pH 7.5, 150 mM KCl and incubated for at least 10 min at room temperature. Bands were visualized by illumination with a UV-light box at 302 nm and detection by using a charge-coupled device camera.

Analytical Ultracentrifugation—Analytical sedimentation equilibrium ultracentrifugation was carried out at 20 °C on a Beckman Optima XL-A analytical ultracentrifuge equipped with absorbance optics and an An60 Ti rotor. The partial specific volume $\bar{v}$ at this temperature was determined from the amino acid composition to be 0.726 $ml\cdot g^{-1}$ for NAP1, 0.746 $ml\cdot g^{-1}$ for the histones, and 0.730 $ml\cdot g^{-1}$ for the NAP1-histone complexes using the program SEDNTERP version 1.05[2] (29). Hydration values of 0.44 g of H_2O per g of NAP1, 0.39 g of H_2O per g of histone, and 0.43 g of H_2O per g of NAP1·histone complex were calculated as described previously (35). Proteins were dialyzed against buffer containing 10 mM Tris-HCl, pH 7.5, 5% (v/v) glycerol and 10 or 100 mM KCl prior to analysis. The density ρ of the buffer was 1.0133 $g\cdot ml^{-1}$ (10 mM KCl) and 1.0176 $g\cdot ml^{-1}$ (100 mM KCl), and the viscosity η was 1.1680 mPa·s (10 mM KCl) and 1.1667 mPa·s (100 mM KCl) at 20 °C as calculated with SEDNTERP.

Sedimentation equilibrium ultracentrifugation runs were performed with NAP1 concentrations ranging between 0.5 and 32 μM and at speeds of 5,000, 7,000, and 10,000 rpm and for some runs also at 3,000 and 15,000 rpm. The NAP1-H2A^f·H2B complexes were studied with 3 μM H2A^f·H2B dimer (6 μM histone monomer) and 6 μM NAP1. In addition, experiments were conducted, in which the NAP1 concentration was varied from 3 to 12 μM. NAP1 and H3·H4^f were mixed at a 1:1 monomer ratio using 8.6 μM H3·H4^f dimer and 17.3 μM NAP1. Equilibrium was obtained after 24–30 h as judged from a comparison of scans recorded at intervals of 4 h. Absorbance data were collected at 230 and 280 nm by averaging 10 scans with radial increments of 0.001 cm in step mode. Absorbance values above 1.3 were not included in the analysis. The sedimentation equilibrium data were analyzed by global fitting of all data sets of a given sample with the software UltraScan version 6.2 (www.ultrascan.uthscsa.edu) from Borries Demeler. A monomer-dimer, dimer-octamer, or dimer-octamer-hexadecamer model was used as described in the text. Other models that involved a NAP1 dimer as basic building block and included tetramers or hexamers were also tested but did not lead to good fits. All fits derived according to Reactions 1–4 had a fit quality of 35% or higher, with a value of >30% being considered as an adequate model for the data.

Analytical sedimentation velocity studies were conducted at 20 °C and at 35,000 and 42,000 rpm in epon double-sector cells and in the same buffer used for the equilibrium runs. The NAP1 concentration was between 1 and 4 μM for the analysis of NAP1 complexes. For experiments with histones 3 μM H2A·H2B dimer (6 μM histone monomer) and 6 μM NAP1 monomer or 20 μM NAP1 and 10 μM H3·H4^f dimer (20 μM histone monomer) were used. Data were collected at 230, 280, or 496 nm using a spacing of 0.03 cm in a continuous scan mode. A global analysis of the sedimentation velocity experiments was conducted with the program SEDPHAT version 2.0 (www.analyticalultracentrifugation.com) (36). The local residual mean square deviation was between 0.006 and 0.011 for single and global fits. The same models as in the equilibrium runs were used with an instantaneous equilibrium between different association states corresponding to kinetic off-rate constants that are equal or faster than 0.1/s.

RESULTS

NAP1 Associates into Dimer, Octamer, and Hexadecamer—Yeast NAP1 was expressed in *Escherichia coli* and purified by His tag affinity and ion exchange chromatography (Fig. 1*A*). A contaminating DNase activity present in the eluate from the nickel-chelating resin was removed by a second chromatography step on a Mono-Q ion exchange column. After the final purification step the protein was more than 95% pure and the preparation had no detectable DNase activity as tested by incubation with supercoiled plasmid substrate at 37 °C over several days and analysis by agarose gel electrophoresis (data not shown). For some AUC experiments the His tag of NAP1 was removed by thrombin digestion to test if the tag effects the association state. The His tag was cut off quantitatively under appropriate conditions with hardly any additional degradation of the protein (Fig. 1*B*). NAP1 preparations equivalent to those obtained after 6–22 h of digestion were used in subsequent AUC experiments.

Binding of NAP1 to histones was studied with histone H2A·H2B and H3·H4 complexes that were reconstituted from overexpressed and purified recombinant histones (30). The heterodimer/tetramer complexes were prepared with the fluorescent dye Alexa 488 covalently attached to either H2A or to H4 in a site-specific manner (see "Experimental Procedures"). These labeled H2A^f or H4^f histones displayed an additional

[2] J. Philo, D. Hayes, and T. Laue, available at www.jphilo.mailway.com/download.htm.

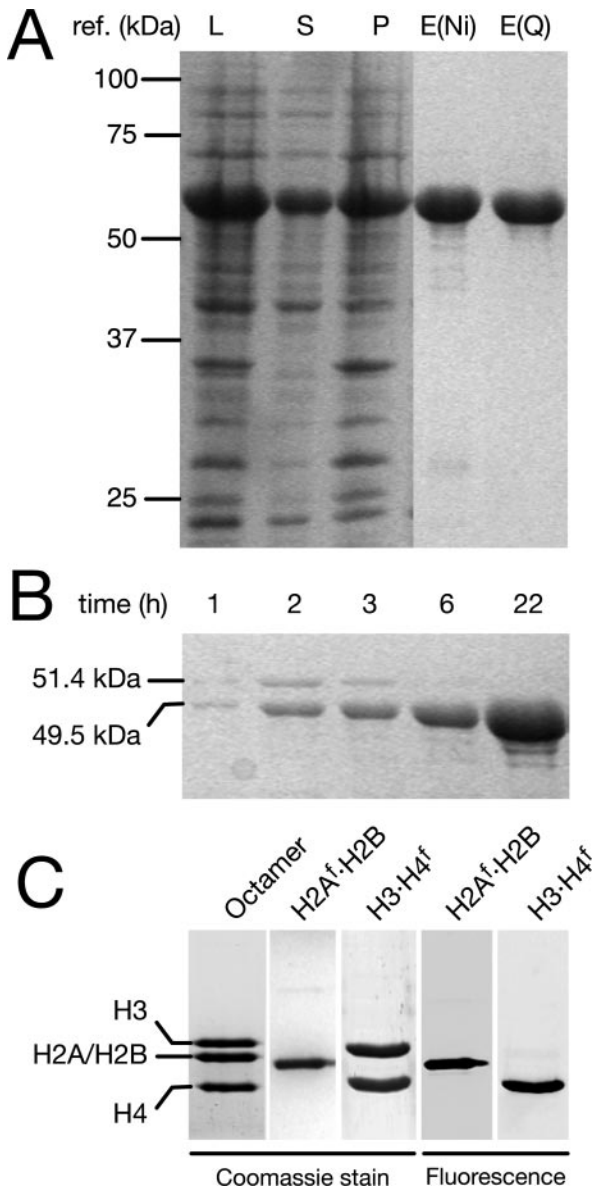

FIG. 1. *A*, purification of NAP1 protein from *E. coli* with nickel-affinity and ion exchange chromatography. Due to its high number of negative charges the NAP1 protein displays a somewhat reduced mobility on SDS gels with an apparent molecular mass of ≈60 kDa. *L*, lysate; *S*, supernatant; *P*, pellet; *E(Ni)*, eluate after affinity purification with nickel-agarose beads; *E(Q)*, eluate from Mono-Q ion exchange column. *B*, cleavage of His tag from NAP1. NAP1 was bound to nickel-agarose beads, and thrombin cleavage was conducted for the times indicated. Increasing amounts of tag-free NAP1 were released to the supernatant. At extended incubation times unspecific cleavage by thrombin resulted in faster moving bands. *C*, gel electrophoretic analysis of reconstituted and purified H2A^f·H2B dimer and (H3·H4^f)$_2$ tetramer. An SDS-gel is shown with visualization of the protein by Coomassie staining in comparison to the H2A^f and H4^f fluorescence signal of the same lanes. As a reference, a histone octamer is included that has been reconstituted from purified recombinant histones as described previously (31). Histones H2A^f and H2B are not separated on the gel.

absorbance maximum at 496 nm and a fluorescence maximum at about 520 nm allowing specific detection of NAP1-histone complexes by absorbance and fluorescence measurements. Fig. 1*C* shows a Coomassie-stained SDS-gel with the purified histone H2A^f·H2B and H3·H4^f complexes and a reconstituted histone octamer preparation as a reference. The SDS-gel demonstrates that the histone preparations are highly purified and that H2A^f and the H4^f displayed the expected fluorescence signal upon excitation of the Alexa 488 fluorophore. The recombinant histones H2A und H2B from *X. laevis* have a very similar mobility under standard electrophoretic conditions and are hardly separated (37).

The association states of NAP1 in absence of histones were determined by sedimentation equilibrium ultracentrifugation. Typical data sets are displayed in Fig. 2(*A* and *B*), and the results are summarized in Table I. Initial runs at approximately physiological salt concentrations (100 mM KCl, 2 mM $MgCl_2$) revealed a complex multispecies equilibrium. To identify the basic building blocks of the NAP1 multimers the salt concentration was varied from 10 mM to 1 M KCl. At 10 mM KCl an excellent fit of the data was obtained over a concentration range from 0.5 to 13.4 μM NAP1 with a monomer-dimer model and a monomer molecular mass constrained to 51.3 kDa as calculated from the amino acid composition (Fig. 2*A*) according to Reaction 1.

$$2\ \mathrm{NAP1} \rightleftarrows (\mathrm{NAP1})_2$$

REACTION 1

A dissociation constant of $K_{d1-2} = 0.2 \times 10^{-6}$ M was determined. At NAP1 concentrations well above the dissociation constant (measurements at 6.7, 8.1, and 13.4 μM) the data could be described well with a single component fit. A molecular mass of 104 ± 4 kDa was obtained with the molecular mass being the only fit parameter and using the calculated values for the partial specific volume $\bar{v} = 0.726\ \mathrm{ml \cdot g^{-1}}$ of NAP1 and a buffer density of $\rho = 1.0133\ \mathrm{g \cdot ml^{-1}}$ (see "Experimental Procedures"). This result is in excellent agreement with the calculated value of 102.7 kDa for the NAP1 dimer. Thus, NAP1 forms a dimer in low salt buffer, which is the building block for the oligomers formed at physiological salt concentrations. This finding confirms a previous study, in which the NAP1 dimer was identified as the basic association state (26). Accordingly, the molecular mass of the NAP1 dimer of 102.7 kDa was used in further experiments as a fixed parameter to determine the higher association states at physiological buffer conditions and in complexes with histones.

At 100 mM KCl concentration the association of NAP1 into larger complexes was evident from a comparison of the molecular weight averages. For example at ≈2 μM protein concentration average values of 81 ± 4 kDa (10 mM KCl) and 169 ± 9 kDa (100 mM KCl) were determined when fitting the data to a single component model. However, in these experiments systematic deviations from a one or two component model were observed in the residuals of the fits, indicating a more complex equilibrium state. A detailed analysis revealed that the data at 100 mM KCl were best described by a dimer-octamer-hexadecamer equilibrium (Reaction 2).

$$8(\mathrm{NAP1})_2 \rightleftarrows 2(\mathrm{NAP1})_8 \rightleftarrows (\mathrm{NAP1})_{16}$$

REACTION 2

Other models that involve the NAP1 dimer as the smallest unit (*e.g.* formation of tetramer or hexamer) did not lead to good fits. Fig. 2*B* shows a representative data set at 100 mM KCl with a fit to a dimer-octamer-hexadecamer equilibrium and the dimer molecular mass constrained to 102.7 kDa. Very good fits to this model were obtained over a concentration range from 0.5 μM to 32 μM NAP1 monomer with data recorded at 230 and 280 nm. Values for the dissociation constant of $K_{d2-8} = (5.8 \pm 3.9) \times 10^{-18}\ \mathrm{M^3}$ and $K_{d8-16} = (1.2 \pm 0.3) \times 10^{-6}$ M were determined. The concentration at which the ratio of NAP1 in the dimeric and octameric state is 1:1 is $(K_{d2-8})^{1/3} = (1.8 \pm 0.4) \times 10^{-6}$ M. At salt concentrations of 150 mM KCl, 100 mM KCl plus 2 mM $MgCl_2$, or 10 mM KCl plus 2 mM $MgCl_2$ (Table I) the data were also best described with a dimer-octamer-hexadecamer equilib-

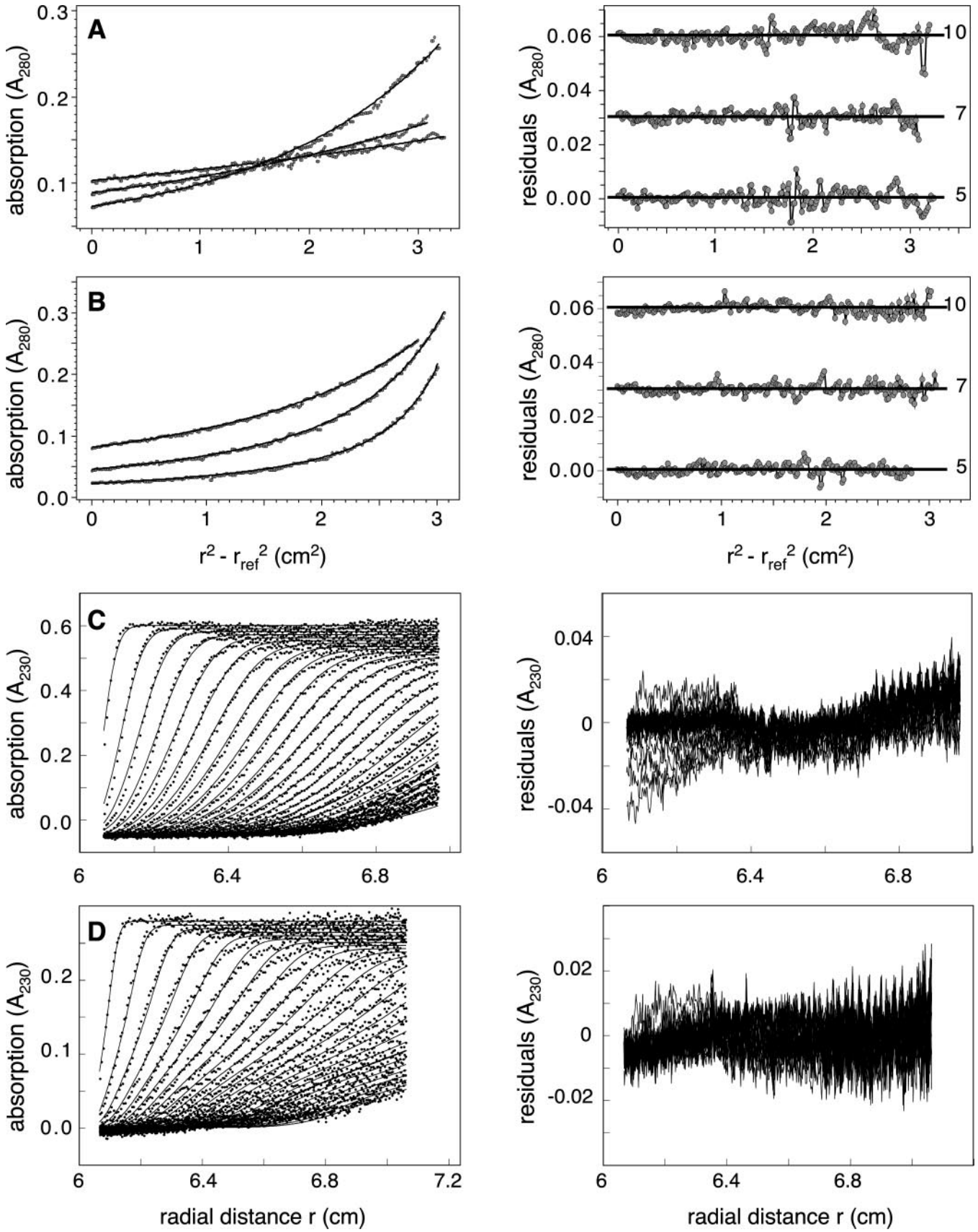

FIG. 2. **Analytical ultracentrifugation of NAP1.** The *left panel* shows the experimental data and the fitted curves in dependence of the radial position. On the *right* the residuals of the fits are plotted. Equilibrium centrifugation experiments were carried out at 20 °C and at 5,000, 7,000, and 10,000 rpm as shown in *A* and *B*. Representative sedimentation velocity runs conducted at 35,000 rpm (*C*) and 42,000 rpm (*D*) are shown with every fifth scan being included in the plot. *A* and *C*, NAP1 in buffer containing 10 mM KCl was fitted with a monomer-dimer equilibrium (Reaction 1) with the molecular mass of the monomer fixed at 51.3 kDa. *B* and *D*, NAP1 in buffer containing 100 mM KCl fitted with a dimer-octamer-hexadecamer equilibrium (Reaction 2).

TABLE I
Association states of NAP1, histones, and NAP1-histone complexes determined by sedimentation equilibrium analysis

KCl (mM)	Basic association state	Abbreviation	M_{fit}[a] (*kDa*)	Equilibrium complexes
10	NAP1 monomer	NAP1	51.3[b]	Monomer·dimer[b]
100	NAP1 dimer	$(NAP1)_2$	102.7	Dimer-octamer-hexadecamer
10 + $MgCl_2$[c]	NAP1 dimer	$(NAP1)_2$	102.7	Dimer-octamer-hexadecamer
100 + $MgCl_2$[c]	NAP1 dimer	$(NAP1)_2$	102.7	Dimer-octamer-hexadecamer
10/100	H2A·H2B dimer	$(H2Af{\cdot}H2B)_1$	28.5[d]	Dimer[d]
10/100	NAP1 dimer with H2A·H2B dimer	$(NAP1)_2$-$(H2A^f{\cdot}H2B)_1$	131.2	Dimer-octamer
10/100	H3·H4 dimer	$(H3{\cdot}H4^f)_1$	27.2[e]	Dimer[e]
10/100	NAP1 dimers with H3·H4 dimer	$(NAP1)_2$-$(H3{\cdot}H4^f)_1$	129.8	Dimer-tetramer-octamer

[a] Molecular masses were fixed in the analysis with equilibrium association models at these values calculated from the amino acid sequence.
[b] A molecular mass of 103.8 ± 1 kDa demonstrating the formation of a dimer was determined from a one component fit for NAP1 at concentrations of 6.7 μM and higher.
[c] $MgCl_2$ was added at a concentration of 2 mM.
[d] A molecular mass of 27.5 ± 4 kDa was determined for H2Af·H2B dimer from measurements at 10 mM and 100 mM KCl with a one-component fit.
[e] Under the conditions of the experiments most of the H3·H4 was present in the dimer state. A molecular mass of 29.7 ± 5 kDa was determined in equilibrium runs at 10 and 100 mM KCl from a one-component fit.

rium with no apparent changes of the dissociation constants. Raising the KCl concentration above 0.5 M led to the dissociation of the complex into increasing amounts of monomeric NAP1 indicating that the formation of the NAP1 dimer involves predominantly electrostatic interactions that are weakened by high salt concentrations. At 500 mM KCl NAP1 was present almost completely as a dimer in agreement with results reported recently (26).

The possible effect of the His tag on the NAP1 association was examined by cleavage of the tag with thrombin (Fig. 1*B*). This construct was studied by equilibrium analytical ultracentrifugation experiments at 100 mM KCl and at NAP1 monomer concentrations of 2, 4, 8, 12, 16, and 32 μM. Within the accuracy of measurement no differences were observed in the average molecular weight or multimer equilibrium distribution (data not shown). Best fits were also obtained with a dimer-octamer-hexadecamer equilibrium and similar dissociation constants as those determined for the His-tagged NAP1. Thus, the His tag had no detectable effect on the association properties of NAP1. Because a significant fraction of the protein was lost during the additional purification after thrombin digestion of NAP1, the subsequent experiments were conducted with His-tagged NAP1.

NAP1 complexes were also studied by sedimentation velocity analysis to determine the sedimentation coefficient and hydrodynamic shape of the complexes. The salt-dependent association of NAP1 was clearly evident in the sedimentation velocity analysis when computing the weight average sedimentation coefficient. At a protein concentration of 2 μM values of 3.8 ± 0.3 S at 10 mM KCl and 6.5 ± 0.6 S at 100 mM KCl were determined. Again the data were indicative of the presence of several species. The sedimentation coefficients of the single components in the NAP1 multispecies equilibrium system according to Reaction 1 or Reaction 2 were determined with the program SEDPHAT from Peter Schuck (36). The resulting values of the sedimentation coefficients *s* measured at 20 °C are given in Table II. Representative sedimentation velocity plots are shown for 10 mM KCl (Fig. 2*C*) and 100 mM KCl (Fig. 2*D*). The sedimentation coefficients of the monomer and dimer were determined at 10 mM KCl using a monomer-dimer equilibrium model (Reaction 1). The monomer had an *s* value of 2.4 ± 0.2 S, whereas the dimer yielded 4.4 ± 0.2 S. At 100 mM KCl a dimer-octamer-hexadecamer equilibrium (Reaction 2) was used and sedimentation coefficients of 11.4 ± 0.8 S (octamer) and 21.3 ± 0.5 S (hexadecamer) were measured.

NAP1 Binds Histones in a 1:1 Stoichiometry—Initial attempts to analyze the association of NAP1 with recombinant histones H2A·H2B and H3·H4 by analytical ultracentrifugation yielded no clear results. The complex dimer-octamer-hexadecamer equilibrium of NAP1 precluded the identification of additional species with bound histones. Therefore, recombinant histone complexes were prepared with the fluorescent dye Alexa 488 covalently attached to either H2A or to H4 in a site-specific manner. These labeled histones $H2A^f$ or $H4^f$ allowed a specific detection of NAP1·histone complexes both by absorbance and fluorescence measurements.

The initial characterization of complex formation of $H2A^f{\cdot}H2B$ and $H3{\cdot}H4^f$ with NAP1 was conducted using electrophoresis mobility shift assays. Increasing amounts of NAP1 were mixed with labeled histone complexes ($H2A^f{\cdot}H2B$ or $H3{\cdot}H4^f$) and analyzed on agarose gels exploiting the $H2A^f$ or $H4^f$ fluorescence signal (Fig. 3). Free histones migrate into the opposite direction due to their highly positive charge. Accordingly, they were not visible in the gel, except for nonspecific, hardly migrating aggregates in samples, in which an excess of histones was present (Fig. 3, *lanes* with 0, 0.4, and 0.8 μM NAP1). Upon addition of NAP1 to histones, a specific complex formed and reached saturation at a ratio of approximately one NAP1 monomer per histone, both for $H2A^f{\cdot}H2B$ (Fig. 3*A*) and $H3{\cdot}H4^f$ (Fig. 3*B*). Thus, one NAP1 protein binds one histone in good agreement with previous studies (25). It is further noted that NAP1-$H2A^f{\cdot}H2B$ and NAP1-$H3{\cdot}H4^f$ complexes migrated at an apparent identical height, indicative for the formation of complexes of similar size and charge.

NAP1 Dimer and Octamer Form Complexes with H2A·H2B Dimers—The AUC analysis was conducted with absorbance data recorded at 496 nm. Thus, only the species containing $H2A^f{\cdot}H2B$ dimer was detected. For the $H2A^f{\cdot}H2B$ dimer alone a molecular mass of 29 ± 4 kDa was determined in equilibrium runs, which is in very good agreement with the 28.5 kDa derived from the amino acid sequence. NAP1 and histone dimer were mixed at different molar ratios. Only at a ratio of one NAP1 monomer per histone monomer a good fit could be obtained with a dimer-octamer model for sedimentation equilibrium and velocity experiments at both 10 mM and 100 mM KCl according to Reaction 3 (Fig. 4).

$$4(NAP1)_2\text{-}(H2A{\cdot}H2B)_1 \rightleftarrows (NAP1)_8\text{-}(H2A{\cdot}H2B)_4$$

REACTION 3

A NAP1 hexadecamer species with $H2A^f{\cdot}H2B$ was not detected in the experiments. Using a dimer-octamer-hexadecamer model did not improve the fit, and the K_{d8-16} values indicated negligible amounts of hexadecamer. Interestingly, already at 10 mM KCl the octamer complex was present, suggesting a stabilization of the NAP1 octamer upon histone binding at this

TABLE II
Hydrodynamic parameters of NAP1 complexes

	s^a	Molecular mass[b]	$f/f_o{}^c$	$D \times 10^{7d}$	Model fit Reaction[a]
	S	*kDa*		$cm^2\ s^{-1}$	
NAP1	2.4 ± 0.2	51.3	1.80 ± 0.16	4.1 ± 0.4	1
$(NAP1)_2$	4.4 ± 0.2	102.6	1.56 ± 0.07	3.8 ± 0.4	1, 2
$(NAP1)_8$	11.4 ± 0.8	410.4	1.52 ± 0.10	2.5 ± 0.2	2
$(NAP1)_{16}$	21.3 ± 0.5	820.8	1.29 ± 0.05	2.3 ± 0.1	2
$(NAP1)_2$-$(H2A{\cdot}H2B)_1$	5.5 ± 0.7	131.1	1.45 ± 0.16	3.8 ± 0.4	3
$(NAP1)_8$-$(H2A{\cdot}H2B)_4$	16.6 ± 2.2	524.4	1.21 ± 0.14	2.8 ± 0.4	3
$(NAP1)_2$-$(H3{\cdot}H4)_1$	5.5 ± 0.7	129.8	1.44 ± 0.16	3.8 ± 0.4	4
$(NAP1)_4$-$(H3{\cdot}H4)_2$	10.9 ± 1.6	259.6	1.15 ± 0.14	3.8 ± 0.5	4
$(NAP1)_8$-$(H3{\cdot}H4)_4$	16.6 ± 2.2	519.2	1.19 ± 0.14	2.9 ± 0.4	4

[a] The sedimentation coefficient at standard conditions (20 °C, H_2O) as determined from single and global fits to models described by Reactions 1–4 as indicated using SEDPHAT. Standard deviations were determined from averaging results from single fits.
[b] Calculated molecular masses are included as a fixed parameter in the analysis of sedimentation velocity runs.
[c] Ratio of the measured friction coefficient f to the friction coefficient f_o of a sphere with the same volume, including hydration.
[d] Diffusion constants at standard conditions (20 °C, H_2O) determined from the friction coefficient (35).

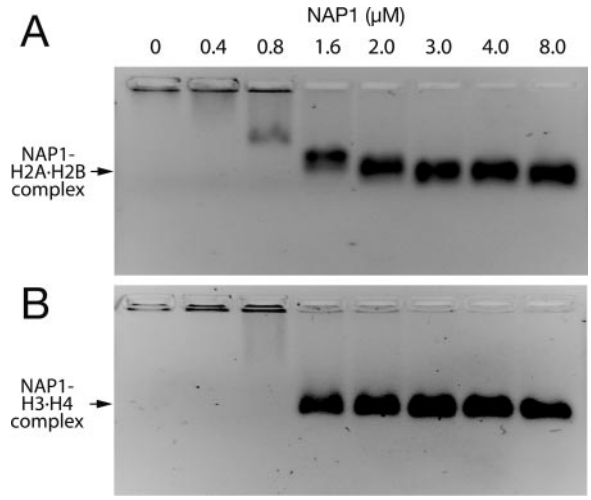

FIG. 3. **Gel shift analysis of NAP1 with the H2A·H2B dimer and the $(H3{\cdot}H4)_2$ tetramer.** *A*, increasing concentrations of NAP1 were mixed with 1.0 μM $H2A^f{\cdot}H2B$ dimer. NAP1 was completely saturated with histones at a ratio of ≈1 NAP1 monomer per histone. *B*, increasing concentrations of NAP1 were mixed with 1.0 μM $H3{\cdot}H4^f$ dimer. At a ratio of ≈1 NAP1 monomer per histone NAP1 was completely saturated with histones.

salt concentration. A value of $K_{d2-8} = 5 \times 10^{-16}$ M^3 and $(K_{d2-8})^{1/3} = 8 \times 10^{-6}$ M was measured. At 100 mM KCl the multimerization occurred with $K_{d2-8} = 3 \times 10^{-18}$ M^3 and $(K_{d2-8})^{1/3} = 1.4 \times 10^{-6}$ M. This is very similar to the NAP1 dimer-octamer equilibrium in the absence of histones showing that the binding of $H2A^f{\cdot}H2B$ dimer had little effect on the formation of the NAP1 octamer at 100 mM KCl. The Histone $H2A^f{\cdot}H2B$ dimer interacted with NAP1 with high affinity, because no indication for the presence of free $H2A^f{\cdot}H2B$ dimer was found at a 1:1 stoichiometry of NAP1 and histone. This is consistent with a NAP1·histone dissociation constant of 20 nM at 0.1 M ionic strength as estimated from affinity blotting experiments (38).

To determine the sedimentation coefficients of the NAP1-$H2A^f{\cdot}H2B$ complexes sedimentation velocity runs were performed and analyzed according to Reaction 3. A representative fit at 10 mM KCl is shown in Fig. 4*C*. The sedimentation coefficient of the $(NAP1)_2$-$(H2A^f{\cdot}H2B)_1$ dimer complex was measured to be 5.5 ± 0.7 S and for the $(NAP1)_8$-$(H2A^f{\cdot}H2B)_4$ octamer complex a value of $s = 16.6 \pm 2.2$ S was determined (Table II).

NAP1 Dimer and Octamer Form Complexes with H3·H4—The analysis of NAP1 complexes in the presence of H3·H4 was also conducted at 496 nm to detect only histone-containing species. For $H3{\cdot}H4^f$ alone a molecular mass of 29.7 ± 5 kDa was determined in equilibrium runs at 10 and 100 mM KCl with a good fit to a one component model. This value is very close to the molecular mass of 27.2 kDa calculated for the dimer, and the fit to a monomer-dimer equilibrium indicated that under these experimental conditions only a small fraction (<15%) associates into the $(H3{\cdot}H4^f)_2$ tetramer. This is consistent with previous studies that reported the dissociation of $(H3{\cdot}H4)_2$ tetramer into dimers at low ionic strength and protein concentration in the micromolar range (39, 40). The formation of a stable $(H3{\cdot}H4)_2$ tetramer would require higher protein and salt concentrations than those used here (40).

NAP1 and histones were mixed in equimolar amounts and examined by sedimentation equilibrium (Fig. 5*A*) and velocity centrifugation (Fig. 5*B*) at 10 mM and 100 mM KCl. All data sets showed a good fit to a dimer-tetramer-octamer model with a fixed molecular mass of 129.8 kDa for the $(NAP1)_2$-$(H3{\cdot}H4^f)_1$ dimer complex as described in Reaction 4.

$$4(NAP1)_2\text{-}(H3{\cdot}H4)_1 \rightleftarrows 2(NAP1)_4\text{-}(H3{\cdot}H4)_2 \rightleftarrows (NAP1)_8\text{-}(H3{\cdot}H4)_4$$

REACTION 4

Thus, $H3{\cdot}H4^f$ behaves very similar to $H2A^f{\cdot}H2B$ in its interaction with NAP1 but in addition to the dimer and octamer complex an association state forms, in which two NAP1 dimers stabilize the $(H3\text{-}H4^f)_2$ tetramer complex. At 10 mM KCl this complex was the prevalent species, and little octamer complex was present, whereas at 100 mM KCl the concentration of the $(NAP1)_4$-$(H3{\cdot}H4^f)_2$ complex was low and the $(NAP1)_8$-$(H3{\cdot}H4^f)_4$ complex formed with a dissociation constant of $K_{d2-8} = 2 \times 10^{-17}$ M^3 and $(K_{d2-8})^{1/3} = 3 \times 10^{-6}$ M.

Sedimentation coefficients for the $(NAP1)_2$-$(H3{\cdot}H4^f)$ and $(NAP1)_8$-$(H3{\cdot}H4^f)_4$ complexes were found to be equivalent to those of the corresponding complexes with $H2A^f{\cdot}H2B$ within the accuracy of the measurement. Accordingly, the values for these association states were averaged resulting in $s = 5.5 \pm 0.7$ S (dimer) and $s = 16.6 \pm 2.2$ S (octamer). The sedimentation coefficient of the $(NAP1)_4$-$(H3{\cdot}H4^f)_2$ complex was determined to be 10.9 ± 1.6 S (Table II).

Conformations of NAP1 Complexes Are Derived from Hydrodynamic Measurements—From the sedimentation coefficients measured for the NAP1 complexes the ratio of the friction coefficient f to that of a sphere with the same volume and friction coefficient f_o was calculated (Table II). The relatively high f/f_o ratios indicate that the conformation of NAP1 dimer and octamer differ significantly from a sphere for which f/f_o would equal one. Upon binding of histones to NAP1 dimer only a small decrease of the friction coefficient ratio was observed from 1.52 ± 0.10 to 1.45 ± 0.16 for the $(NAP1)_2$-$(H2A{\cdot}H2B)_1$

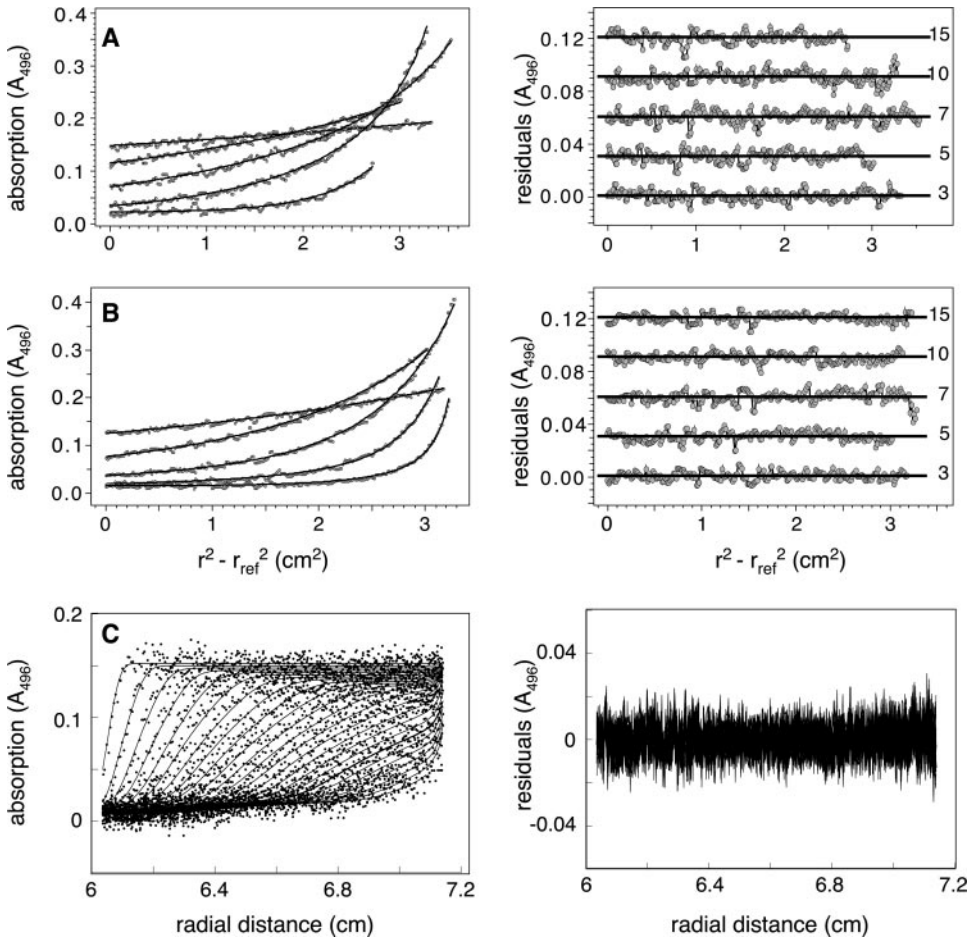

FIG. 4. **Analytical ultracentrifugation of NAP1 complexes with histone $H2A^f$·H2B dimer.** Experiments were recorded at 496 nm. The *left panel* shows the experimental data and the fitted curves in dependence of the normalized radial position. On the *right* the residuals of the fits are plotted. Runs were fitted to the model given in Reaction 3 with the molecular mass of the $(NAP1)_2$-$(H2A{\cdot}H2B)_1$ species constrained to 131.2 kDa. Data acquired at 10 mM KCl (*A*) and 100 mM KCl (*B*) are shown. *C*, sedimentation velocity run at 10 mM and a NAP1/histone ratio of 1:1. Only every fifth scan is shown.

and to 1.44 ± 0.16 for the $(NAP1)_2$-$(H3{\cdot}H4)_1$ species. In contrast the NAP1 octamer complex adopted a more globular shape when associated with histones, because the value of f/f_o decreased significantly. In analogy to the stacked annular pentamer-decamer structure formed by the histone chaperone nucleoplasmin (9, 10, 41) we propose the model depicted in Fig. 6*A*. It is consistent with the hydrodynamic parameters derived from the sedimentation velocity analysis, but it is noted also that other arrangements of NAP1 subunits would be compatible with the measured friction coefficient ratios. In our model the NAP1 octamer forms an annular structure, which can stack to form a hexadecamer. The disk-shaped structure of the depicted octamer has a relatively high friction coefficient, and stacking of two octamers would lead to a reduction of the f/f_o ratio as observed in the sedimentation velocity runs, which yielded values of $f/f_o = 1.52 \pm 0.10$ (octamer) and $f/f_o = 1.29 \pm 0.05$ (hexadecamer) (Table II). Upon histone binding the NAP1 octamer undergoes a transition to a more compact association state as indicated in Fig. 6*A* by an accompanying decrease of the central cavity.

The friction coefficients and the known molecular weights can be used to calculate the diffusion constant *D*. The values for *D* in pure water are listed in Table II. From mobility measurements of other proteins like GFP it is estimated that in the cell the corresponding *in vivo* value would be 3 to 4 times lower due to the higher viscosity in the absence of any topological constraints to the mobility imposed by chromatin or other cellular structures (42).

NAP1 Octamer Formation Could Be Induced in Vivo during S Phase by NAP1 Accumulation in the Nucleus—The number of NAP1 monomers in haploid yeast cells has been determined to be around 8070 molecules in microarray experiments (43). During G_1 phase NAP1 is mostly excluded from the nucleus (21, 44). A haploid yeast cell has an average cell volume of 32 μm^3 (45). Estimating that about half of the cell volume is occupied by organelles like nucleus, vacuole, mitochondria, and the Golgi apparatus that are inaccessible to NAP1 this would correspond to a concentration of ≈1 μM NAP1 monomer or ≈0.5 μM NAP1 dimer. From the dissociation constants K_{d2-8} and K_{d8-16} determined in the AUC experiments it can be concluded that during G_1 phase NAP1 is present in the cytoplasm mostly as a dimer. As plotted in Fig. 6*B* the fraction of NAP1 present in the dimer, octamer, and hexadecamer state would be 94:6:0.1%.

During S phase dephosphorylation of NAP1 leads to its accumulation in the nucleus (14, 19) with some increase in the expression level (18) resulting in a significantly higher NAP1 concentration. The yeast nucleus has a total volume of ~3.6 μm^3 of which not more than 2.9 μm^3 are estimated to be accessible for NAP1 (46, 47). Without considering any increase in the expression level a concentration of 4 μM NAP1 monomer could be reached if 80% of NAP1 would be localized in the nucleus. This would favor the association of NAP1 dimer into octamer and hexadecamer. For a 2 μM NAP1 dimer concentration the ratio of dimer:octamer:hexadecamer is 50:38:12% (Fig. 6*B*). Taking into consideration that upon histone binding the

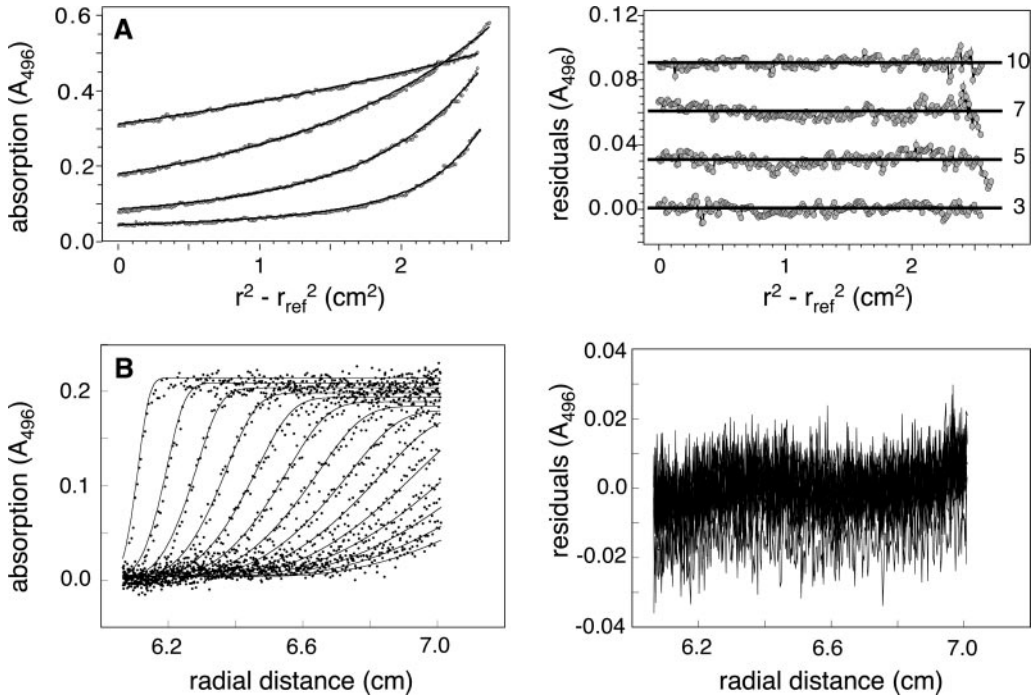

FIG. 5. **Analytical ultracentrifugation of NAP1 complexes with histone $(H3{\cdot}H4^f)_2$ tetramer.** Experiments were recorded at 496 nm. The *left panel* shows the experimental data and the fitted curves in dependence of the normalized radial position. On the *right* the residuals of the fits are plotted. Equilibrium runs were fitted to the model given in Reaction 4 with the molecular mass of the $(NAP1)_2$-$(H3{\cdot}H4^f)_1$ species constrained to 129.8 kDa. The data sets shown were acquired at 100 mM KCl by equilibrium sedimentation (*A*) and velocity sedimentation (*B*), where only every fifth scan is shown.

hexadecamer was destabilized and not detected in the AUC experiments the fraction of NAP1 in dimeric and octameric complexes would be 53:47%.

DISCUSSION

NAP1 mediates various important biological activities like the rearrangement of nucleosomes during transcription, the shuttling of the histone H2A·H2B dimer from the cytoplasm to the nucleus, and the assembly of newly synthesized DNA into chromatin (see Refs. 5–7, 10 for reviews). These diverse functions of NAP1 are likely to differ with respect to the number and type of histones found in complexes with NAP1. An understanding of the different NAP1 association states is therefore an essential prerequisite for any mechanistic studies of NAP1 activities. Considerable efforts have been made to characterize the multimer equilibrium of NAP1 alone and in complexes with histones (13, 14, 23, 25, 26). However, the physiologically relevant association states adopted by NAP1 remained to be elucidated. Here analytical ultracentrifugation was used to identify the complexes of NAP1 alone and with core histones, and to characterize these with respect to their thermodynamic stability and hydrodynamic shape.

The NAP1 monomer was only observed at unphysiologically low ionic strength and associates into a dimer with high affinity if the salt concentration is raised. At physiological ionic strength an equilibrium between NAP1 dimer, octamer, and hexadecamer was present (Table I). The measured sedimentation coefficients of the monomer (2.4 ± 0.2 S) and dimer (4.4 ± 0.2 S) determined in our analysis are in good agreement with the values measured recently in the presence of 500 mM KCl and 1.8 M guanidinium hydrochloride (26). In addition, a NAP1 octamer and hexadecamer were identified here with *s* values of 11.4 ± 0.8 and 21.3 ± 0.5 (Table II). The data summarized in Tables I and II lead to the model shown in Fig. 6*A*, in which the NAP1 dimer associates into a disk-shaped annular octamer. The hexadecamer is formed by stacking two octamers on top of each other. This conformation is consistent with the large reduction of the friction coefficient ratio from f/f_o = 1.52 ± 0.10 (octamer) to f/f_o = 1.29 ± 0.05 (hexadecamer). Because these conformations are similar to the pentamer-decamer structure formed by the histone chaperone nucleoplasmin (9, 10, 41), they appear the most likely, although other shapes and arrangements of NAP1 subunits would also be compatible with the observed friction coefficient ratios.

The interactions between NAP1 and core histones were investigated first in gel shift experiments, and a stoichiometry of 1:1 for NAP1-histone complexes was measured, which confirms the results reported previously (25). The NAP1-histone complexes have been described to sediment between 5 and 12 S (13, 14, 23, 24). Here, the species that predominantly form under physiological salt and protein concentrations were identified as a NAP1 dimer bound to a histone dimer (5.5 ± 0.7 S) and a NAP1 octamer-histone complex (16.6 ± 2.2 S) (Table II). No significant shifts in the equilibrium between the NAP1 dimer and the NAP1 octamer were observed upon histone binding under these conditions.

Based on AUC results and estimates of the intracellular concentration of NAP1 the model shown in Fig. 7 was devised for the cell cycle-dependent formation of different NAP1 association states. During transcription chromatin regions have to adopt a more open conformation. Removal of one H2A·H2B dimer from the histone octamer seems to be essential for transcription elongation through nucleosomes (48, 49), and NAP1 and other histone chaperones stimulate the binding of transcription factors to chromatin templates (50, 51). In addition, the histone H2A·H2B dimer exchanges more rapidly than the H3·H4 tetramer *in vivo* (52, 53). It has been shown that NAP1 is present in complexes with SWR1 that catalyzed the exchange of H2A·H2B dimer to a dimer variant in yeast (54). Thus, as shown in Fig. 7, mediating the dissociation and rebinding of single H2A·H2B dimers during transcription in G_1 phase is a likely function of NAP1 dimers that could explain its effect on gene expression (15). During DNA replication in S

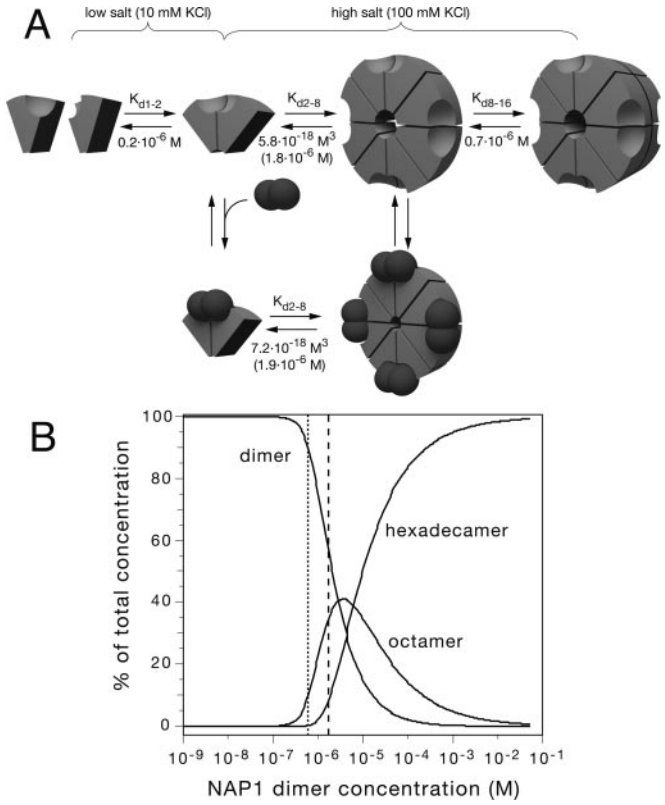

FIG. 6. *A*, model of association states of NAP1. At low salt concentration (10 mM KCl) NAP1 is present as a monomer and a dimer. At higher salt concentration (100 mM) the smallest association state is the NAP1 dimer. This associates further to an octamer and a hexadecamer with the indicated K_d values. The values in *parentheses* refer to $(K_{d2-8})^{1/3}$, the concentration at which the ratio of NAP1 in the dimeric and octameric state is 1:1. The K_d values for multimerization of complexes with histones are similar to those of free NAP1. However, no hexadecamer was detected in the presence of histones. The NAP1 octamer-histone complex adopts a more compact conformation than the free NAP1 octamer as inferred from the hydrodynamic analysis. H3·H4 behaves essentially as H2A·H2B except for an additional intermediate complex formed predominantly at 10 mM KCl as described in Reaction 4. *B*, dependence of the three NAP1 species on total NAP1 concentration. At 1 μM NAP1 monomer concentration the protein is mostly present as a dimer with a ratio of dimer:octamer:hexadecamer of 94:6:0.1 (*dotted line*). In contrast, at around 4 μM NAP1 monomer half of the protein is in larger complexes with relative dimer:octamer:hexadecamer fractions of 50:38:12 (*dashed line*).

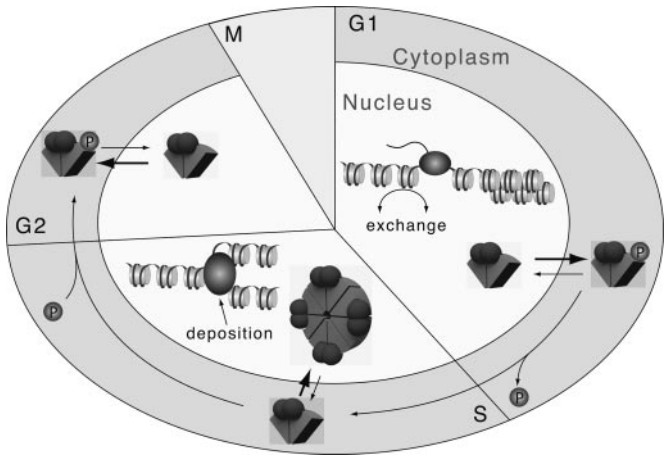

FIG. 7. **Hypothetical model for the cell cycle-dependent association states of NAP1.** During G_1 phase NAP1 is mainly phosphorylated and thus cytoplasmic. Low concentrations of NAP1 present as dimers in the nucleus participate in chromatin rearrangement during transcription regulation and bind free H2A·H2B dimers. For this function a dimer that can carry the H2A·H2B dimer would be sufficient. During transition into S phase NAP1 is dephosphorylated and accumulates in the nucleus leading to higher concentrations. This induces the association of NAP1 into the octameric state, which is able to carry multiple H2A·H2B dimers and possibly also H3·H4 dimers to the replication sites. At the end of S phase NAP1 gets phosphorylated again, is exported to the cytoplasm, and dissociates to a dimer.

phase histones are needed in large quantities in the nucleus. Upon dephosphorylation during the G_1/S transition NAP1 shuttles histones into the nucleus (14, 19–21, 55). In some cases also a higher expression of NAP1 was observed during S-phase (16, 18). Due to the accumulation of NAP1 in the nucleus its local concentration increases, leading to a significant increase of the NAP1 octamer complex fraction (Fig. 6*B*). Based on these results, it is estimated that for a concentration of 2 μM NAP1 dimer in the nucleus ~50% would be present in the octamer complex. The actual fraction of the NAP1 octamers might be higher *in vivo* due to excluded volume effects that are referred to as macromolecular crowding (56). Furthermore, the NAP1 dimer-octamer equilibrium could be directly affected by post-translational modifications like polyglutamylation (57), phosphorylation, or acetylation. Acetylation of NAP1 by p300 was shown to promote its ability to assemble chromatin and facilitates the transfer of H2A·H2B from nucleosomes to NAP1. Acetylation occurs in a cell cycle-dependent manner (19, 58) suggesting a possible regulatory function in histone binding and complex assembly. Here it is proposed that during S-phase the nuclear NAP1 complex is present mostly as an octamer (Figs. 6 and 7). This complex has eight histone binding sites, which could facilitate the *de novo* assembly of nucleosomes by binding two H2A·H2B dimers and two H3·H4 dimers, sufficient for the assembly of a complete histone octamer. It is noted that the *in vitro* experiments presented here and in the literature show high affinity binding of NAP1 to all core histones (13, 14, 23–25). However, an *in vivo* interaction of NAP1 with histones H3·H4 has not been demonstrated and only NAP1-H2A·H2B complexes have been isolated by immunoprecipitation experiments (11, 14, 22). This suggests that the NAP1 interaction with H3·H4 is prevented by the association of H3·H4 dimers with histone chaperone CAF-1 (5, 39, 59) and/or DNA. However, NAP1 is sufficient for the *in vitro* assembly of nucleosomes and can serve as a carrier for all four core histones in the reaction (60). This process is of considerable interest for the reconstitution of chromatin with defined histone composition. It is also conceivable that the NAP1-mediated assembly of complete nucleosomes is taking place *in vivo* under specific conditions that remain to be identified.

In summary, NAP1 has various important activities like the import of H2A·H2B into the nucleus and the assembly of two H2A·H2B dimers and possibly also H3·H4 into nucleosomes during replication. Furthermore, it interacts with the histone H2A·H2B dimer during transcription and histone exchange. These processes differ with respect to the number of histones involved. Thus, the quantitative description of the association states of NAP1 alone and in complexes with histones presented here provides new insights into the mechanisms by which NAP1 can exert its different biological functions.

Acknowledgments—The support of Peter Lichter is gratefully acknowledged. We thank Felix Kepert, Malte Wachsmuth, Lutz Ehrhardt, and Borries Demeler for help and Tamas Fischer for valuable discussions. We are grateful to Karolin Luger, Gernot Laengst, and Tom Owen-Hughes for providing plasmid vectors. The project was supported by the Volkswagen Foundation in the program "Junior Research Groups at German Universities."

REFERENCES

1. Arents, G., Burlingame, R. W., Wang, B.-C., Love, W. E., and Moudrianakis, E. N. (1991) *Proc. Natl. Acad. Sci. U. S. A.* **88,** 10148–10152
2. Luger, K., Mäder, A. W., Richmond, R. K., Sargent, D. F., and Richmond, T. J.

(1997) *Nature* **389,** 251–260
3. Davey, C. A., Sargent, D. F., Luger, K., Maeder, A. W., and Richmond, T. J. (2002) *J. Mol. Biol.* **319,** 1097–1113
4. Harp, J. M., Hanson, B. L., Timm, D. E., and Bunick, G. J. (2000) *Acta Crystallogr. D Biol. Crystallogr.* **56,** 1513–1534
5. Loyola, A., and Almouzni, G. (2004) *Biochim. Biophys. Acta* **1677,** 3–11
6. Tyler, J. K. (2002) *Eur. J. Biochem.* **269,** 2268–2274
7. Adams, C. R., and Kamakaka, R. T. (1999) *Curr. Opin. Genet. Dev.* **9,** 185–190
8. Haushalter, K. A., and Kadonaga, J. T. (2003) *Nat. Rev. Mol. Cell. Biol.* **4,** 613–620
9. Prado, A., Ramos, I., Frehlick, L. J., Muga, A., and Ausio, J. (2004) *Biochem. Cell Biol.* **82,** 437–445
10. Akey, C. W., and Luger, K. (2003) *Curr. Opin. Struct. Biol.* **13,** 6–14
11. Nakagawa, T., Bulger, M., Muramatsu, M., and Ito, T. (2001) *J. Biol. Chem.* **276,** 27384–27391
12. van Holde, K. E. (1989) *Chromatin*, p. 416, Springer, Heidelberg
13. Ishimi, Y., Hirosumi, J., Sato, W., Sugasawa, K., Yokota, S., Hanaoka, F., and Yamada, M. (1984) *Eur. J. Biochem.* **142,** 431–439
14. Ito, T., Bulger, M., Kobayashi, R., and Kadonaga, J. T. (1996) *Mol. Cell. Biol.* **16,** 3112–3124
15. Ohkuni, K., Shirahige, K., and Kikuchi, A. (2003) *Biochem. Biophys. Res. Commun.* **306,** 5–9
16. Dong, A., Zhu, Y., Yu, Y., Cao, K., Sun, C., and Shen, W. H. (2003) *Planta* **216,** 561–570
17. Zimmerman, Z. A., and Kellogg, D. R. (2001) *Mol. Biol. Cell* **12,** 201–219
18. Mortensen, E. M., McDonald, H., Yates, J., 3rd, and Kellogg, D. R. (2002) *Mol. Biol. Cell* **13,** 2091–2105
19. Asahara, H., Tartare-Deckert, S., Nakagawa, T., Ikehara, T., Hirose, F., Hunter, T., Ito, T., and Montminy, M. (2002) *Mol. Cell. Biol.* **22,** 2974–2983
20. Rodriguez, P., Munroe, D., Prawitt, D., Chu, L. L., Bric, E., Kim, J., Reid, L. H., Davies, C., Nakagama, H., Loebbert, R., Winterpacht, A., Petruzzi, M. J., Higgins, M. J., Nowak, N., Evans, G., Shows, T., Weissman, B. E., Zabel, B., Housman, D. E., and Pelletier, J. (1997) *Genomics* **44,** 253–265
21. Miyaji-Yamaguchi, M., Kato, K., Nakano, R., Akashi, T., Kikuchi, A., and Nagata, K. (2003) *Mol. Cell. Biol.* **23,** 6672–6684
22. Chang, L., Loranger, S. S., Mizzen, C., Ernst, S. G., Allis, C. D., and Annunziato, A. T. (1997) *Biochemistry* **36,** 469–480
23. Ishimi, Y., Sato, W., Kojima, M., Sugasawa, K., Hanaoka, F., and Yamada, M. (1985) *Cell Struct. Funct.* **10,** 373–382
24. Fujii-Nakata, T., Ishimi, Y., Okuda, A., and Kikuchi, A. (1992) *J. Biol. Chem.* **267,** 20980–20986
25. McBryant, S. J., Park, Y. J., Abernathy, S. M., Laybourn, P. J., Nyborg, J. K., and Luger, K. (2003) *J. Biol. Chem.* **278,** 44574–44583
26. McBryant, S. J., and Peersen, O. B. (2004) *Biochemistry* **43,** 10592–10599
27. Laue, T. M., and Stafford, W. F., 3rd. (1999) *Annu. Rev. Biophys. Biomol. Struct.* **28,** 75–100
28. Lebowitz, J., Lewis, M. S., and Schuck, P. (2002) *Protein Sci.* **11,** 2067–2079
29. Laue, T. M., Shah, B. D., Ridgeway, T. M., and Pelletier, S. L. (1992) in *Analytical Ultracentrifugation in Biochemistry and Polymer Science* (Harding, S. E., Rowe, A. J., and Horton, J. C., eds) pp. 90–125, Royal Society of Chemistry, Cambridge
30. Luger, K., Rechsteiner, T. J., and Richmond, T. J. (1999) *Methods Enzymol.* **304,** 3–19
31. Kepert, J. F., Fejes Tóth, K., Caudron, M., Mücke, N., Langowski, J., and Rippe, K. (2003) *Biophys. J.* **85,** 4012–4022
32. Lee, K. M., and Hayes, J. J. (1997) *Proc. Natl. Acad. Sci. U. S. A.* **94,** 8959–8964
33. Bruno, M., Flaus, A., Stockdale, C., Rencurel, C., Ferreira, H., and Owen-Hughes, T. (2003) *Mol. Cell* **12,** 1599–1606
34. Haugland, R. P. (2004) *Handbook of Fluorescent Probes and Research Chemicals*, 9th Ed., pp. 20–36, Molecular Probes, Eugene, OR
35. Rippe, K., Mücke, N., and Schulz, A. (1998) *J. Mol. Biol.* **278,** 915–933
36. Schuck, P. (2003) *Anal. Biochem.* **320,** 104–124
37. Luger, K., Rechsteiner, T. J., Flaus, A. J., Waye, M. M., and Richmond, T. J. (1997) *J. Mol. Biol.* **272,** 301–311
38. McQuibban, G. A., Commisso-Cappelli, C. N., and Lewis, P. N. (1998) *J. Biol. Chem.* **273,** 6582–6590
39. Tagami, H., Ray-Gallet, D., Almouzni, G., and Nakatani, Y. (2004) *Cell* **116,** 51–61
40. Baxevanis, A. D., Godfrey, J. E., and Moudrianakis, E. N. (1991) *Biochemistry* **30,** 8817–8823
41. Dutta, S., Akey, I. V., Dingwall, C., Hartman, K. L., Laue, T., Nolte, R. T., Head, J. F., and Akey, C. W. (2001) *Mol. Cell* **8,** 841–853
42. Wachsmuth, M., Waldeck, W., and Langowski, J. (2000) *J. Mol. Biol.* **298,** 677–689
43. Ghaemmaghami, S., Huh, W. K., Bower, K., Howson, R. W., Belle, A., Dephoure, N., O'Shea, E. K., and Weissman, J. S. (2003) *Nature* **425,** 737–741
44. Rodriguez, P., Pelletier, J., Price, G. B., and Zannis-Hadjopoulos, M. (2000) *J. Mol. Biol.* **298,** 225–238
45. Johnston, G. C., Ehrhardt, C. W., Lorincz, A., and Carter, B. L. (1979) *J. Bacteriol.* **137,** 1–5
46. Ostashevsky, J. (2002) *Mol. Biol. Cell* **13,** 2157–2169
47. Weidemann, T., Wachsmuth, M., Knoch, T. A., Muller, G., Waldeck, W., and Langowski, J. (2003) *J. Mol. Biol.* **334,** 229–240
48. Studitsky, V. M., Walter, W., Kireeva, M., Kashlev, M., and Felsenfeld, G. (2004) *Trends Biochem. Sci.* **29,** 127–135
49. Belotserkovskaya, R., Oh, S., Bondarenko, V. A., Orphanides, G., Studitsky, V. M., and Reinberg, D. (2003) *Science* **301,** 1090–1093
50. Walter, P. P., Owen-Hughes, T. A., Cote, J., and Workman, J. L. (1995) *Mol. Cell. Biol.* **15,** 6178–6187
51. Chen, H., Li, B., and Workman, J. L. (1994) *EMBO J.* **13,** 380–390
52. Kimura, H., and Cook, P. R. (2001) *J. Cell Biol.* **153,** 1341–1353
53. Levchenko, V., and Jackson, V. (2004) *Biochemistry* **43,** 2359–2372
54. Mizuguchi, G., Shen, X., Landry, J., Wu, W. H., Sen, S., and Wu, C. (2004) *Science* **303,** 343–348
55. Li, M., Strand, D., Krehan, A., Pyerin, W., Heid, H., Neumann, B., and Mechler, B. M. (1999) *J. Mol. Biol.* **293,** 1067–1084
56. Ellis, R. J. (2001) *Trends Biochem. Sci* **26,** 597–604
57. Regnard, C., Desbruyeres, E., Huet, J. C., Beauvallet, C., Pernollet, J. C., and Edde, B. (2000) *J. Biol. Chem.* **275,** 15969–15976
58. Ito, T., Ikehara, T., Nakagawa, T., Kraus, W. L., and Muramatsu, M. (2000) *Genes Dev.* **14,** 1899–1907
59. Smith, S., and Stillman, B. (1989) *Cell* **58,** 15–25
60. Ito, T., Levenstein, M. E., Fyodorov, D. V., Kutach, A. K., Kobayashi, R., and Kadonaga, J. T. (1999) *Genes Dev.* **13,** 1529–1539

Association States of Nucleosome Assembly Protein 1 and Its Complexes with Histones

Katalin Fejes Tóth, Jacek Mazurkiewicz and Karsten Rippe

J. Biol. Chem. 2005, 280:15690-15699.
doi: 10.1074/jbc.M413329200 originally published online January 31, 2005
